AD-A113 936 COLD REGIONS RESEARCH AND ENGINEERING LAB HANOVER NH F/G 20/12
CHARGED DISLOCATION IN ICE. II. CONTRIBUTION OF DIELECTRIC RELA--ETC(U)
MAR 82 K ITAGAKI
UNCLASSIFIED CRREL-82-7 NL

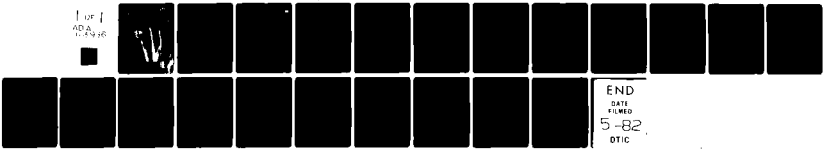

END
DATE FILMED
5-82
DTIC

CRREL
REPORT 82-7

US Army Corps
of Engineers
Cold Regions Research &
Engineering Laboratory

12

Charged dislocation in ice
II. Contribution of dielectric relaxation

82 04 28 011

For conversion of SI metric units to U.S./ British customary units of measurement consult ASTM Standard E380, Metric Practice Guide, *published by the American Society for Testing and Materials, 1916 Race St., Philadelphia, Pa. 19103.*

Cover: X-ray diffraction topograph of ice single crystal showing dislocations. (Photograph by K. Itagaki.)

CRREL Report 82-7

March 1982

Charged dislocation in ice
II. Contribution of dielectric relaxation

Kazuhiko Itagaki

Prepared for
OFFICE OF THE CHIEF OF ENGINEERS

Unclassified

SECURITY CLASSIFICATION OF THIS PAGE *(When Data Entered)*

REPORT DOCUMENTATION PAGE		READ INSTRUCTIONS BEFORE COMPLETING FORM
1. REPORT NUMBER CRREL Report 82-7	2. GOVT ACCESSION NO. AD-A113 936	3. RECIPIENT'S CATALOG NUMBER
4. TITLE *(and Subtitle)* CHARGED DISLOCATION IN ICE: II. CONTRIBUTION OF DIELECTRIC RELAXATION		5. TYPE OF REPORT & PERIOD COVERED 6. PERFORMING ORG. REPORT NUMBER
7. AUTHOR(s) Kazuhiko Itagaki		8. CONTRACT OR GRANT NUMBER(s)
9. PERFORMING ORGANIZATION NAME AND ADDRESS U.S. Army Cold Regions Research and Engineering Laboratory Hanover, New Hampshire 03755		10. PROGRAM ELEMENT, PROJECT, TASK AREA & WORK UNIT NUMBERS DA Project 4A161102AT24, Task C, Work Unit 002
11. CONTROLLING OFFICE NAME AND ADDRESS Office of the Chief of Engineers Washington, D.C. 20314		12. REPORT DATE March 1982 13. NUMBER OF PAGES 21
14. MONITORING AGENCY NAME & ADDRESS*(if different from Controlling Office)*		15. SECURITY CLASS. *(of this report)* Unclassified 15a. DECLASSIFICATION/DOWNGRADING SCHEDULE
16. DISTRIBUTION STATEMENT *(of this Report)* Approved for public release; distribution unlimited.		
17. DISTRIBUTION STATEMENT *(of the abstract entered in Block 20, if different from Report)*		
18. SUPPLEMENTARY NOTES		
19. KEY WORDS *(Continue on reverse side if necessary and identify by block number)* Dielectric strength Dislocation Electric charge Ice Single crystals		
20. ABSTRACT *(Continue on reverse side if necessary and identify by block number)* The contribution of electrically charged dislocation motion to dielectric relaxation was studied theoretically. Experimentally obtained data on charge density, dislocation density, and segment length and distribution described in Part I of this series were used to calculate dielectric relaxation spectra. The results indicate that the charged dislocation process can produce the observed audio frequency dielectric relaxation as well as the distribution of spectra.		

DD FORM 1 JAN 73 1473 EDITION OF 1 NOV 65 IS OBSOLETE

Unclassified

SECURITY CLASSIFICATION OF THIS PAGE *(When Data Entered)*

PREFACE

This report was prepared by Dr. Kazuhiko Itagaki, Research Physicist, of the Snow and Ice Branch, Research Division, U.S. Army Cold Regions Research and Engineering Laboratory. Funding for this research was provided by DA Project 4A161102AT24, *Research in Snow, Ice and Frozen Ground*, Task C, *Research in Terrain and Climatic Constraints*, Work Unit 002, *Adhesion and Physics of Ice*.

The author thanks Dr. Steven Arcone and Dr. William St. Lawrence of CRREL for technical review of the manuscript, Dr. A. Granato of the University of Illinois for his very helpful discussions, and Dr. A. von Hippel and Dr. W.B. Westphal of the Massachusetts Institute of Technology for their continuous interest.

CONTENTS

ILLUSTRATIONS

TABLES

CHARGED DISLOCATION IN ICE
II. Contribution of dielectric relaxation

Kazuhiko Itagaki

INTRODUCTION

Many theoretical and experimental studies concern the dielectric relaxation of ice (Hobbs 1974). The coincidence of dielectric relaxation time with activation energies and the relaxation time of internal friction has been attributed to the rearrangement of protons through the Bjerrum defect (Bjerrum 1951).

A study by von Hippel et al. (1972) indicates that the relaxation spectrum may contain up to seven dielectric relaxation times. Three of them, with peaks at about 20 kHz and 2 kHz in the -21°C range, and 20 to 50 Hz at -10°C, generally agree with our measurements. Also, two spectra of internal friction relaxation time have been found by Kuroiwa (1965) and also by VanDevender and Itagaki (1973). Both internal friction spectra seem to agree with two dielectric relaxation spectra of higher frequency within a factor of 1.5 to 2, depending on dislocation structure.

The effects of mechanical treatment on dielectric relaxation of ice observed by us (to be published in subsequent reports in this series) show behavior similar to the results of internal friction relaxation in the range of our measurements. All previously published results were made with heavily strained ice so that reasonable comparison with our strain-free samples may not be possible.

The complicated dielectric relaxation of ice, especially the effect of mechanical treatment, cannot be explained by simple Bjerrum defect theory. Charged dislocations, as discussed in Part I of this series, can be displaced by an electric field which, in turn, contributes to electric polarization and then to the dielectric constant and relaxation. Many of the properties of the dielectric relaxation and internal friction results currently attributed to the Bjerrum defect may possibly be explained by charge dislocation theory. This report will present a theoretical study of dielectric relaxation caused by charged dislocations. Although the basic concept was discussed by the present author (Itagaki 1969) and by Brantley and Bauer (1969), further developments have enabled us to make a more detailed examination.

THEORETICAL DEVELOPMENT OF DIELECTRIC RELAXATION DUE TO CHARGED DISLOCATIONS

The model for charged dislocation motion is an electrically charged string of linear mass A stretched by tension C in a viscous medium having a resistance factor B. The lateral displacement η at point x can be described by the equation of a vibrating string:

$$A \frac{\partial^2 \eta}{\partial t^2} + B \frac{\partial \eta}{\partial t} - C \frac{\partial^2 \eta}{\partial x^2} = E_0' \mu e^{i\omega t} \qquad (1)$$

where ω is the angular velocity, μ is the linear charge density of the dislocation, and the amplitude of the total field E_0' is the sum of the applied field E_0 and the local field caused by dielectric polarization acting on the dislocation. This equation and the following treatment is parallel to the

dislocation damping theory by Koehler (1952) and Granato and Lücke (1956) except that the stress field is replaced by an electric field and strain is replaced by polarization. The solution of this equation for the boundary conditions $\eta = 0$ at $x = 0$ and $x = \ell$ is

$$\eta = \frac{4\mu E_0'}{A} \sum_{n=0}^{\infty} \frac{1}{2n+1} \sin \frac{(2n+1)\pi x}{\ell} \frac{\exp[i(\omega t - \delta_n)]}{[(\omega_n^2 - \omega^2)^2 + (\omega d)^2]^{1/2}} \tag{2}$$

where

$d = B/A$

$A = \pi \rho b^2$

b = the Burgers vector

ρ = crystal density

ℓ = the dislocation segment length

$$\omega_n = (2n+1)\frac{\pi}{\ell}\left(\frac{C}{A}\right)^{1/2}$$

$$\delta_n = \tan^{-1}\frac{\omega d}{\omega_n^2 - \omega^2} .$$

The line tension C is given as

$$C = 2K_s b^2/\pi$$

where K_s is the energy factor (Hirth and Lothe 1968).

Polarization P due to a displaced charged dislocation of segment length ℓ is

$$P = \mu \bar{\eta} \ell$$

where mean displacement

$$\bar{\eta} = \frac{1}{\ell}\int_0^{\ell} \eta(x)\, dx$$

$$= \frac{4\mu E_0'}{A\ell} \sum \frac{1}{2n+1} \frac{\exp[i(\omega t - \delta n)]}{[(\omega_n^2 - \omega^2) + (\omega d)^2]^{1/2}} \int_0^{\ell} \sin \frac{(2n+1)}{\ell} \pi x\, dx$$

$$= \frac{8\mu E_0'}{\pi A \ell} \sum \frac{1}{(2n+1)^2} \frac{\exp[i(\omega t - \delta n)]}{[(\omega_n^2 - \omega^2)^2 + (\omega d)^2]^{1/2}} . \tag{3}$$

By definition, the dielectric permittivity κ due to the polarization caused by the charged dislocations for the uniform segment length ℓ distributed in a volume V is

$$\kappa = 1 + \frac{P}{\epsilon_v E} = 1 + \frac{\mu}{\epsilon_v E}\int_v \bar{\eta}\ell\, dv .$$

where ϵ_v is the dielectric constant of a vacuum.

Then for applied field $E = E_0 \exp i\omega t$

$$\kappa = 1 + \int_v \frac{8\mu^2 E_0'}{\pi A \epsilon_v E_0 \exp(i\omega t)} \sum_n \frac{1}{(2n+1)^2} \cdot \frac{\exp[i(\omega t - \delta n)]}{[(\omega_n^2 - \omega^2)^2 + (\omega d)^2]^{1/2}}\, dv$$

$$= 1 + \frac{8\mu^2 \ E_0'}{\pi A \epsilon_v E_0} \int_\nu \sum_n \frac{\exp(-i\delta n)}{(2n+1)^2} \cdot \frac{d\nu}{[(\omega_n^2 - \omega^2)^2 + (\omega d)^2]^{1/2}} . \tag{4}$$

For a uniform segment length of L and dislocation density Λ we obtain as a first approximation

$$\kappa = 1 + \frac{8\mu^2 \Lambda E_0'}{\pi A \epsilon_v E_0} \ \frac{\exp(-i\delta_0)}{[(\omega_0^2 - \omega^2)^2 + (\omega d)^2]^{1/2}}$$

$$\delta_0 = \tan^{-1} \frac{\omega d}{\omega_0^2 - \omega^2} \ . \tag{5}$$

Because $\kappa = \kappa' - i\kappa''$ and $\exp(-i\delta_0) = \cos\delta_0 - i \sin\delta_0$ where

$$\cos\delta = \frac{1}{\sqrt{1 + \tan^2\delta}} = \frac{\omega_0^2 - \omega^2}{\sqrt{(\omega_0^2 - \omega^2)^2 + \omega^2 d^2}}$$

and

$$\sin\delta = \frac{\tan\delta}{\sqrt{1 + \tan^2\delta}} = \frac{\omega d}{\sqrt{(\omega_0^2 - \omega^2)^2 + \omega^2 d^2}}$$

we obtain

$$\kappa' = 1 + \frac{8\mu^2 \Lambda E_0'}{\pi A \epsilon_v E_0} \ \frac{\omega_0^2 - \omega^2}{(\omega_0^2 - \omega^2)^2 + \omega^2 d^2} \ . \tag{6a}$$

and

$$\kappa'' = \frac{8\mu^2 \Lambda E_0'}{\pi A \epsilon_v E_0} \ \frac{\omega d}{(\omega_0^2 - \omega^2)^2 + (\omega d)^2} \ . \tag{6b}$$

Since $\omega_0 = (\pi/L)(C/A)^{1/2}$ is on the order of 10^8 but the measurements were made in the range of $\omega < 6 \times 10^5$, further approximation

$$\kappa' = 1 + \frac{8\mu^2 \Lambda L^2 E_0'}{\pi^3 C \epsilon_v E_0} \ \frac{1}{1 + \omega^2 \tau^2} \tag{7a}$$

$$\kappa'' = \frac{8\mu^2 \Lambda L^2 E_0'}{\pi^3 C \epsilon_v E_0} \ \frac{\omega\tau}{1 + \omega^2 \tau^2} \tag{7b}$$

can be justified where

$$\tau = \frac{BL^2}{\pi^2 C} \ .$$

Equations 7a and b indicate that the relaxation is of a Debye type if the segment length is uniform throughout the crystal. Note that the slope of the κ' vs κ''/ω relationship, which is the dielectric relaxation time of this string model, coincides with τ, the relaxation time of the vibrating string. The contribution of charged dislocation polarization to the static dielectric permittivity κ_0' is found from eq 7a by setting $\omega = 0$; thus

$$\kappa_0' = 1 + \frac{8\mu^2 \Lambda L^2 E_0'}{\pi^3 C \epsilon_v E_0} . \qquad (8)$$

As discussed in Part I, we have obtained the following information required to make a numerical calculation from X-ray topographs:

$$\mu_{max} = 1.5 \times 10^{-10} \text{ C/m}$$
$$\mu_{prob} = 5 \times 10^{-11} \text{ C/m}$$
$$\mu_{min} = 3.2 \times 10^{-12} \text{ C/m}$$
$$\Lambda = 5 \times 10^{8}/\text{m}^2$$
$$L = 7.6 \times 10^{-4} \text{ m}.$$

C can be theoretically calculated from

$$C = 2b^2 K_s/\pi = 4.16 \times 10^{-10} N .$$

Various assumptions were made to estimate the total field E_0' for the derivation of charge density μ. It is difficult to calculate the field in the geometry of the specimen, which is a thin slab having its electric field parallel to the largest surface used in the charge density measurements. The maximum charge density μ_{max} of 1.5×10^{-10} C/m was derived by assuming that $E_0' = (\kappa_0' + 1) E_0/2$ (Itagaki 1979). The usually observed dielectric permittivity of unstrained ice is roughly 90, which will give us $E_0' = 45.5 \times E_0$, yielding μ_{min} of 3.2×10^{-12} C/m. Under the conditions of the charge density measurements discussed in Part I, dislocations under observation were located in the low dislocation density area in the thin slab of ice. We could disregard the effects of nearby dislocations for the first approximation in such a case. By using the dielectric permittivity $\kappa_0' = 5$ of dislocation-free ice (Itagaki 1978), $E_0' = 3E_0$, and we obtain a value of μ_{prob} of 5×10^{-11}C/m.

If we assume that the same total field for the geometry of the thin slab used in the charge density measurements is applicable to the dielectric measurements, we obtain κ_0' as shown in column 2 of Table 1. In the bulk of the crystal having κ_0' of 90 we have obtained $E_0'/E_0 = 45.5$. Column 4 of the Table 1 indicates the calculated dielectric permittivities using this total field relationship.

Table 1. Charge density vs calculated static dielectric permittivity κ_0'.

Charge density	κ_0' *Thin slab*	E_0'/E_0	κ_0' *Bulk ice*	E_0'/E_0
μ_{max} 1.5×10^{-10} C/m	456.4	1	20,721	45.5
μ_{prob} 5×10^{-11}	152.8	3	2,303	45.5
μ_{min} 3.2×10^{-12}	10.4	45.4	10.4	45.5

The dislocation density of carefully prepared Mendenhall glacier ice is on the order of $5 \times 10^{8}/\text{m}^2$, which agrees with Fukuda and Higashi (1969). The usual practice of sample preparation for dielectric measurement involves mechanical cutting and sanding which would increase the dislocation density by several orders of magnitude. X-ray diffraction topography is useless for ice with such a high dislocation density. The low value of the calculated κ_0' does not mean that the charged dislocation mechanism cannot be responsible for the observed dielectric permittivity. The dislocation density of a sample that has undergone normal mechanical treatment may suffice to produce the observed value of κ_0', the static dielectric permittivity. Some of the strain-free prepared samples in dielectric measurements indicated anomalously low values of κ_0' values, supporting this notion.

A higher charge density may create an anomalously high κ_0' value. However, the dislocation density observed by the X-ray topography method used for this calculation was not only the density of the mobile dislocations responsible for dielectric relaxation, but included immobile dislocations as well. Interestingly the dislocation density required to create the observed internal friction peak using the theory of Granato and Lücke (1956) is usually several orders of magnitude lower than that obtained from direct measurements.

Calculation of the total field E_0' requires knowledge of the depolarization, which is difficult to calculate in the linear configuration as dislocation. However E_0' would never be lower than the applied field E_0, and therefore the present estimation is the minimum value for the local field. Since κ_0' is sensitive to μ and L, for which accurate values are difficult to obtain from X-ray topography, it is unfortunately subject to a rather large error. The value of κ_0' calculated here indicated, however, that charged dislocations can contribute a large enough dielectric relaxation to be considered as one of the major mechanisms.

It may be interesting to note that if the total field E_0' is the combination of the applied field and modified Mosotti field as discussed in Appendix A of Part I, a Mosotti type of catastrophe may result from the dislocation process. Further discussion is given in Appendix A of the present report. The problem of which spectra are caused by charged dislocation processes still remains. Some of the six peaks of a relaxation spectrum that von Hippel et al. (1973) identified should be due to charged dislocation processes, but which ones? Are all the peaks real? May part of a spectrum be due to the segment length distribution? The following study sheds light on some of these questions.

NUMERICAL CALCULATIONS FOR DISTRIBUTED SEGMENT LENGTH

Equations 7a and b were modified to account for the effect of distributed segment length by substituting $\tau = B\ell^2/\pi^2 C$ as

$$\kappa' = 1 + \frac{8\mu^2 E_0'}{\epsilon_v \pi^3 C E_0} \int_0^\infty \frac{\ell^2 N(\ell)}{1 + \omega^2 \ell^4 \left(\frac{B}{\pi C}\right)^2} \, d\ell \tag{9a}$$

$$\kappa'' = \frac{8\mu^2 B E_0'}{\epsilon_v \pi^5 C^2 E_0} \int_0^\infty \frac{\ell^4 N(\ell) \omega}{1 + \omega^2 \ell^4 \left(\frac{B}{\pi^2 C}\right)^2} \, d\ell \, . \tag{9b}$$

Three types of hypothetical segment length distribution were studied numerically,

$$N(\ell) = \frac{\Lambda}{\sigma\sqrt{2\pi}} \exp\left\{\frac{-(\ell - L)^2}{2\sigma^2}\right\} \text{ (normal distribution)}$$

$$N(\ell) = \frac{\Lambda}{\sigma\sqrt{2\pi}} \exp \frac{-\ln(\ell/L)^2}{2\sigma^2} \text{ (log-normal distribution)}$$

and

$$N(\ell) = \left(\frac{\lambda}{L^2}\right) \exp\left(\frac{-\ell}{L}\right) \text{ (distribution derived by Koehler for randomly arranged pinning points)}$$

where L is the mean of segment length and σ is the standard deviation of the distribution.

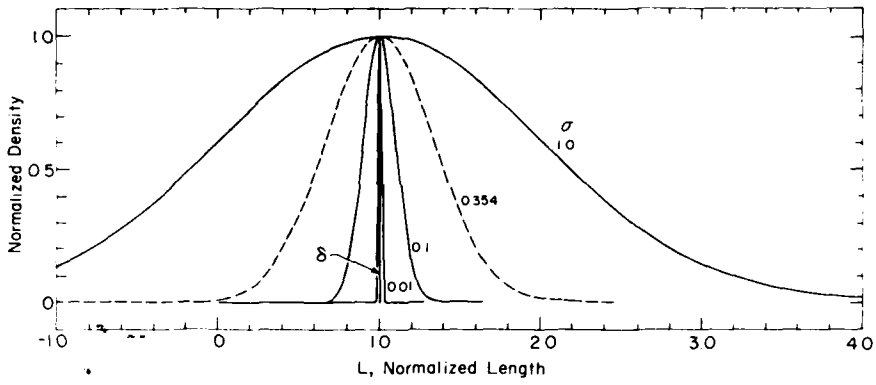

a. Normal distribution having standard deviations of 0.01, 0.1, 0.354, and 1.0. Dashed curve (σ = 0.354) designates results of X-ray topograph measurements.

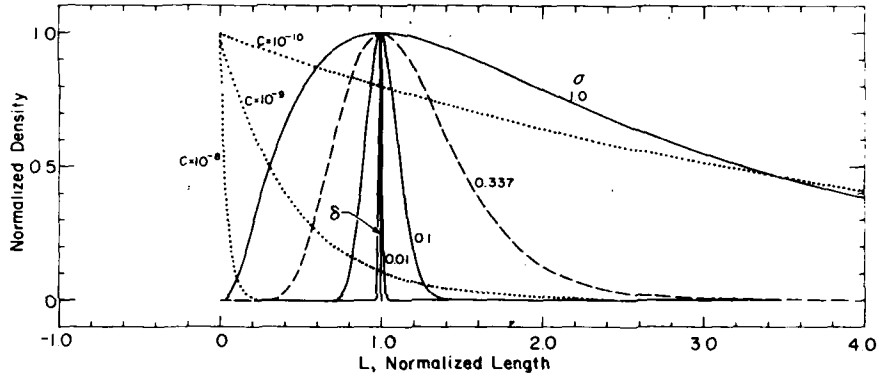

b. Log-normal distribution having standard deviations of 0.01, 0.1, 0.337, and 1.0. Dashed curve (σ = 0.337) designates the results of X-ray topograph measurements. Dotted curves are Koehler's distribution having pinning point densities of 10^{-8}, 10^{-9}, and 10^{-10}. Note that all heights were adjusted to unity.

Figure 1. Probability density curves.

A series of numerical calculations with various parameters were made to determine the effect of segment length distribution on the shapes of Cole-Cole plots and the shift of the peak frequency in plots of κ'' vs frequency. The results are shown in Figures 1-4. When compared to equivalent mean segment lengths in a δ distribution (which has a uniform segment length in these calculations), all other distributions indicate larger and flatter semicircles and peak frequencies that are shifted lower. Also the shape of κ'' vs frequency plot depends on the shape of the distribution.

Since the contributions of longer segments are more pronounced, the size of the Cole-Cole semicircle becomes larger as the distribution becomes wider. This effect occurs even if the distribution is made to have the same mean segment length as the δ distribution.

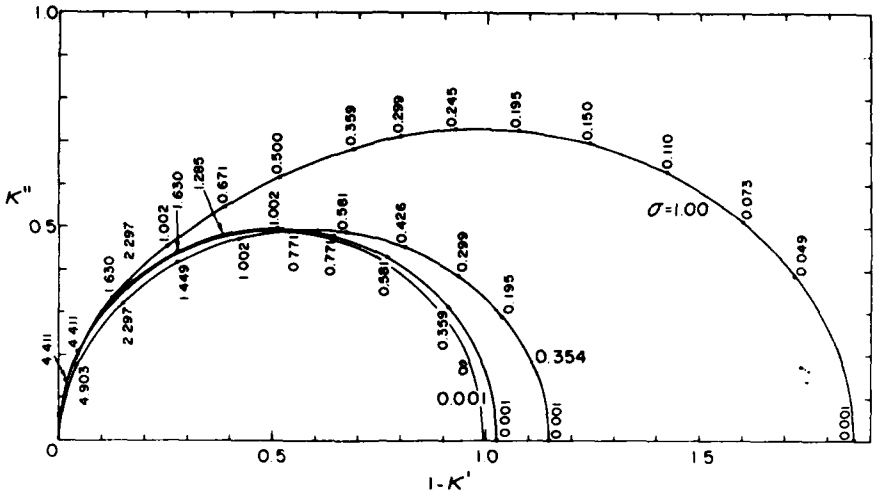

a. Cole-Cole plot (numbers along the curves indicate normalized frequencies).

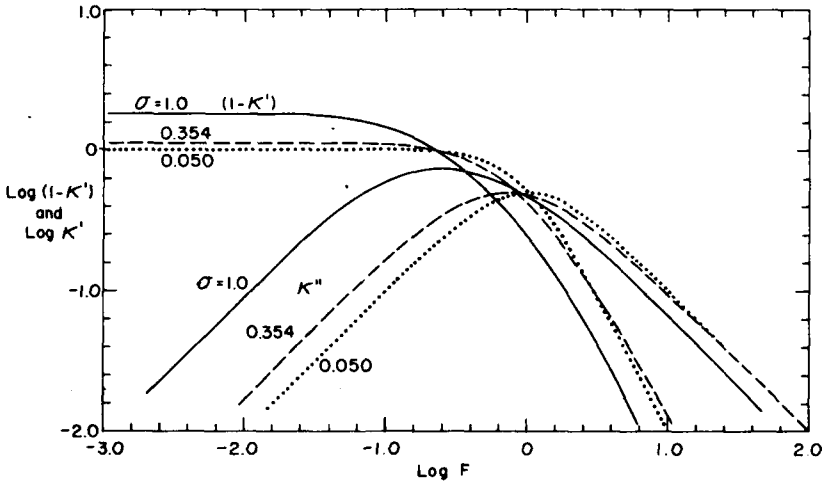

b. Normalized log frequency vs log (1-κ') and log κ'' plot. No detectable difference in shape from the δ distribution is observed for lower standard deviations.

Figure 2. Dielectric relaxation produced by charged dislocations having a normal distribution of segment length (σ = 0.001, 0.354, and 1.0).

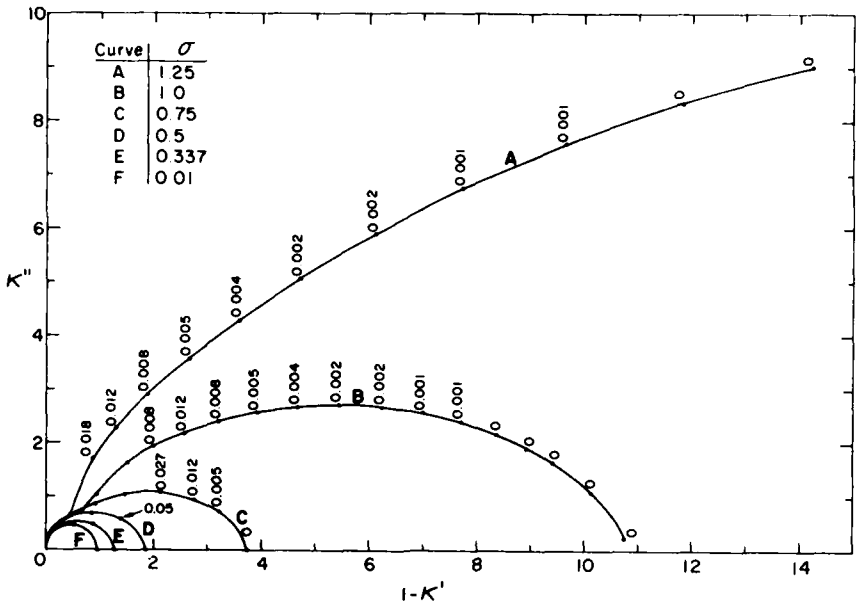

a. Cole–Cole plot.

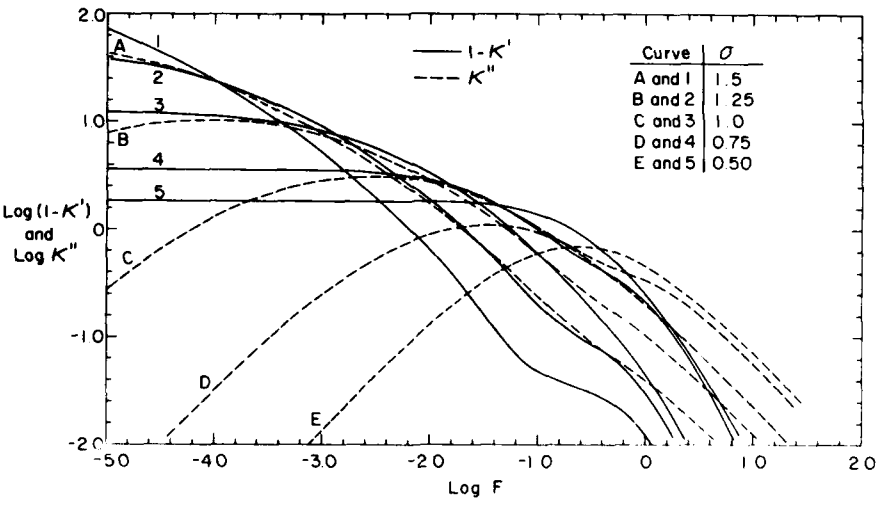

b. Normalized log frequency vs log (1-κ') and log κ" plot. No detectable difference from normal distributions is observed for lower standard deviations.

Figure 3. Dielectric relaxation produced by charged dislocations having a log-normal distribution of segment length (σ = 0.01, 0.337, 0.5, 0.75, 1.0, and 1.25).

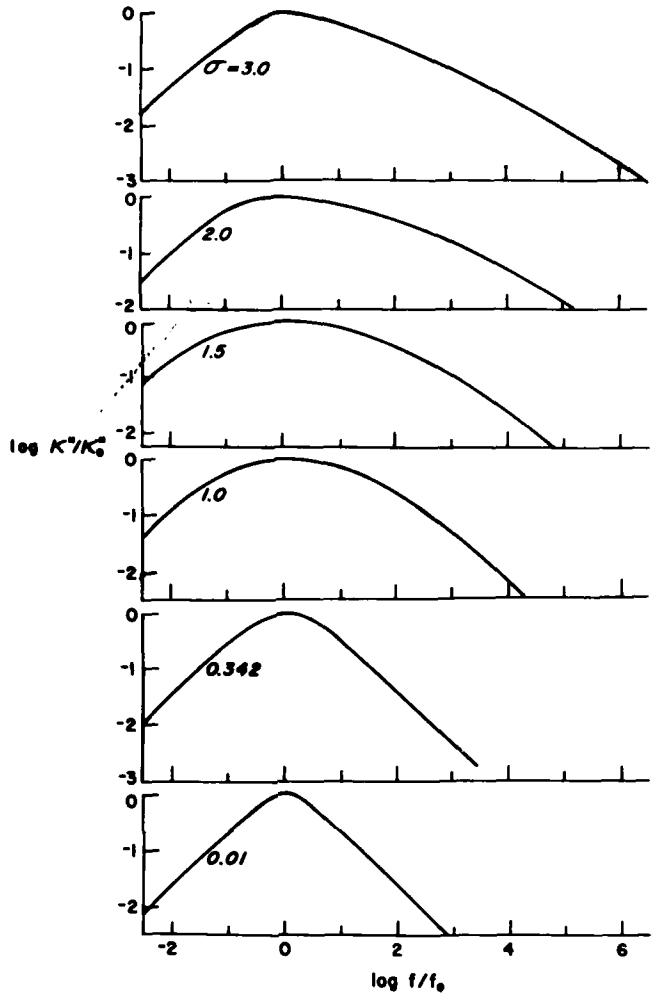

Figure 4. Normalized log frequency vs log κ'' plot of log-normal distribution of segment length. The curves have been moved to make the peak positions coincide.

For the normal distribution of segment length, computations were made for the standard deviations of 0.01, 0.1, 0.354 and 1.0, where a standard deviation of 0.354 is the measured value from an X-ray topograph. The peaks of the segment length distribution were shifted to unity from zero as shown in Figure 1a. Since the density of a negative length segment, a meaningless quantity, becomes significant at values of σ greater than 0.5, the normal distribution is not suitable for a realistic approach for wider segment length distributions. Cole-Cole plots and frequency vs κ' and κ'' plots of corresponding dielectric relaxations shown in Figures 2a and b indicate that a semicircle using the standard deviation of 0.354 generally agrees with the previous measurements of the center depression of 3° to 5°. The apparent relaxation time (usually calculated from the frequency at the highest point of the Cole-Cole plot) is mostly controlled by the contribution of the longer segment length part of the wider distribution. Frequencies normalized to the relaxation time calculated for the δ distribution are shown along the data points on the curve as shown in Figures 2a and 3a. When

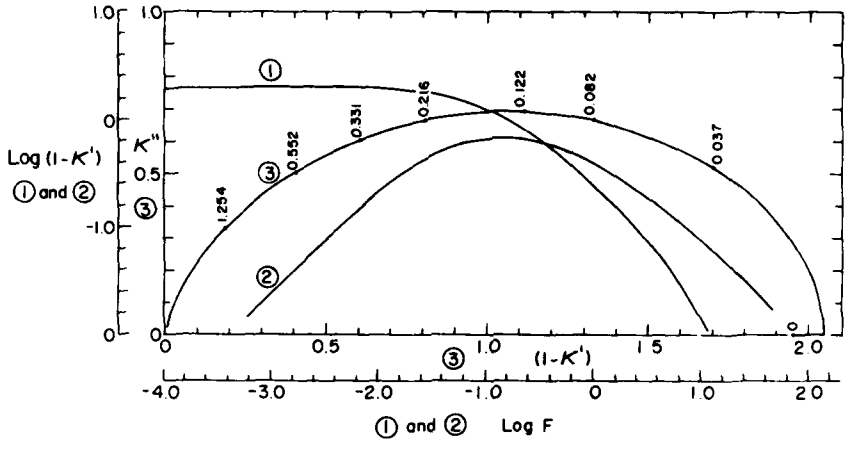

Figure 5. Cole-Cole plot and logarithm of normalized frequency vs log (1-κ') and log κ'' for the Koehler distribution having a pinning point density of 4×10^{-10}. Numbers along the Cole-Cole plot are the frequencies normalized to the relaxation frequency $\omega = 10^5$ which is a close approximation of that observed on ice at around -10°C.

the distribution is very narrow (0.001 in this case) the frequency at the highest point of the Cole-Cole plot is virtually the same as the relaxation frequency. However, the apparent relaxation frequency, defined as the frequency at the highest point of the Cole-Cole plot, becomes smaller as the standard deviation becomes larger. For the relatively narrow distribution of $\sigma = 0.354$ for the normal distribution, the frequency at the highest point becomes 0.581 of the real relaxation frequency for the δ distribution, making the apparent relaxation time longer than the relaxation time for the δ distribution by 1.71. One should be aware of such phenomena when relaxation time is determined by the conventional peak of κ'' method.

The log-normal distribution, especially for a large standard deviation, extends the longer side of the segment length distribution as shown in Figure 1a. Since κ' is proportional to the square and κ'' is proportional to the fourth power of the segment length (eq 9a and 9b), the contribution of the longer segment becomes dominant for the larger σ, making the size of a Cole-Cole plot excessively large (Fig. 3a). From the X-ray topography study (Part I) $\sigma = 0.337$ was obtained by assuming that the distribution is log-normal. No appreciable difference can be observed on the Cole-Cole plot for this range of σ when either the distribution is normal or log normal*.

As σ becomes larger and the distribution becomes wider, the Cole-Cole semicircle becomes flatter and deviates more from the arc of a circle (Fig. 3a). Shifts of many decades in frequency and changes in height of the relaxation peaks are observed in the frequency vs loss plots of Figure 3b. Note that the slope of the lower frequency side changes little, but that the slope of the higher frequency side of the slope becomes less steep and the peaks become wider as σ becomes larger. These features become more easily noticeable when all peaks are normalized to have the same position as shown in Figure 4. Such features resemble those of other dielectric materials discussed by Jonscher (1975). Charged dislocation processes may also be responsible for dielectric and mechanical relaxation of some other materials.

The distribution derived by Koehler may deserve special consideration because the segment length distribution is given under the assumption that the dislocations are pinned by atoms of im-

*An analysis of the shape of the internal friction peak also yielded a reasonably agreeable width, as will be discussed in Part IV of this series.

purities randomly distributed along the dislocation line. Unlike the normal and log-normal distribution treated in this section, Koehler's distribution was derived by using the definite theoretical mechanism of pinning rather than by statistical distribution. Therefore if the results of analysis do not agree with the measurements, we can positively reject the pinning mechanism based on Koehler's assumption. Figure 5 indicates that the Cole-Cole plot was an extensively flat shape which has never been observed in ice, an indication that the distribution of the segment length is not of Koehler's type. Koehler's distribution is a simple exponential for which the contribution of the longer segments does not diminish as quickly as that of a normal or log-normal distribution. An interesting observation to be noted here is that the shapes of the Cole-Cole plots generated by Koehler's distribution remain unchanged regardless of the pinning point density although their size varies widely.

Since the shape of Cole-Cole semicircles is insensitive to the change in σ when σ is small, it is dangerous to conclude that the relaxation is of the Debye type because the measured results lie almost on the semicircle. An a.c. conductance vs permittivity plot is more sensitive as von Hippel et al. (1971) have shown. However, this plot only indicates that the relaxation deviated from that of a Debye type.

DISCUSSION

Frequently dielectric relaxation spectra of ice are said to be an example of Debye relaxation. However, close examination of the Cole-Cole plots indicates that the center of the semicircle is depressed about 3° to 5° from the abscissa in most cases. Depression of the centers in theoretical curves, using the measured standard deviation (0.354 for a normal distribution or 0.337 for a log-normal distribution) as shown in Figures 2a and 3a, is about 5°, agreeing with the direct measurements of the Cole-Cole plot.

The cumulative frequency of measurement segment length was plotted on normal and log-normal probability papers to determine which type of distribution gave the better fit to the measured distribution. Although the number of the data points was limited to 17 and the plot deviated considerably from linear, a log-normal distribution seems to give a better fit than the normal distribution. The plot of log-normal distribution of the experimental data is shown in Figure 6 by filled circles.

Measurements made by Bilde-Sörensen (1973) on deformed MgO indicated that the distribution is heavily skewed towards the shorter segment length. When cumulative distribution density was plotted on log-normal probability paper, all points lay close to a straight line (as shown in Figure 6 by open circles), indicating that the distribution is log-normal. Their distribution ($\sigma = 0.85$) was considerably wider than that of our measurements ($\sigma = 0.337$) made on ice. Previous straining and differences in crystallographic systems probably caused the difference.

Hanson and Morris (1975) made theoretical studies of segment length distribution by assuming that dislocations under stress were pinned by pinning points randomly distributed on a glide plane (shown in Fig. 6 by closed boxes). Their studies were further refined by Labusch (1977) (open boxes in Fig. 6). Both results indicated that the distributions were considerably skewed toward the shorter side of the segment length. Plotting on log-normal probability paper, however, did not yield straight lines, which indicates that assumptions used for their studies did not agree with the measurements made on ice and MgO.

The following relationship may be one of the tests for identifying a charged dislocation mechanism from a point defect mechanism. The static dielectric constant κ_0' can be described as

$$\kappa_0' = 1 + \frac{8\mu^2 \Lambda L^2 E_0'}{\pi^3 C \epsilon_v E_0} \tag{10}$$

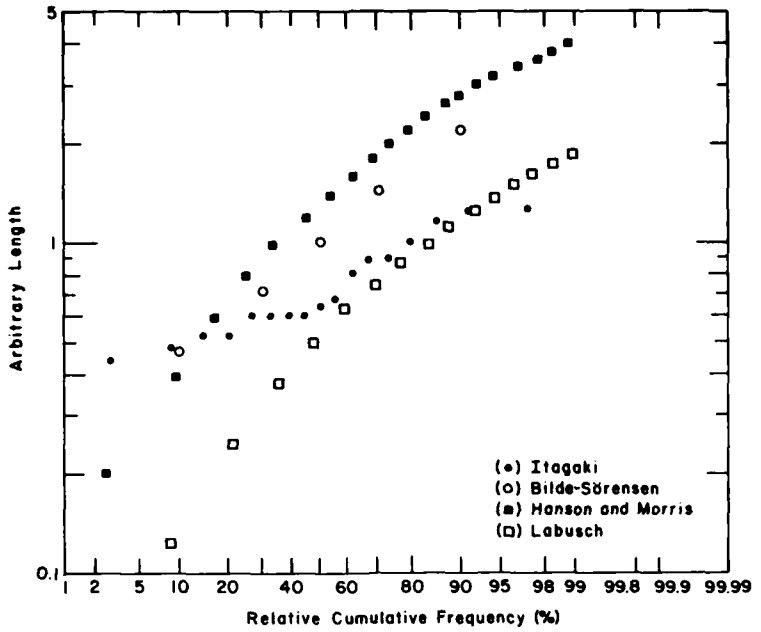

Figure 6. Observed and theoretical calculations of cumulative dislocation segment length distributions plotted on log-normal probability paper. Filled circles are the results of observations made by this author using the X-ray topography method on ice single crystals. Open circles are the results of theoretical calculations by Hanson and Morris (1975) and by Labusch (1977) respectively. Observed points lie on straight lines while theoretical points do not.

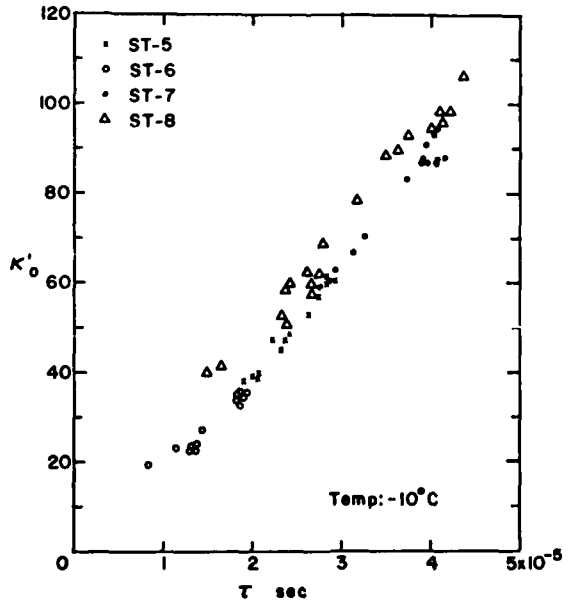

Figure 7. Linear relationship between τ and κ'_0 by shear straining.

from eq 7a assuming $\omega = 0$. Letting $\tau = BL^2/\pi^2 C$, then

$$\kappa_0' = 1 + 8\tau \frac{\mu^2 \Lambda E_0'}{B\epsilon_v E_0 \pi} \quad . \tag{11}$$

Therefore, τ and κ_0' have a linear relationship through L as a parameter which can be modified by deformation. Straining would lengthen the mean segment length L by unpinning until the dislocation source is put into work. The examples shown in Figure 7 show that most of the spectra have linear relationships, indicating that these spectra are produced by a charged dislocation process (a detailed description of this will be given in Part III). However, deviation from linearity does not necessarily indicate a noncharged dislocation process. Dislocation density Λ may start to increase with straining to make the κ_0' vs τ relationship nonlinear or irreversible.

All point defect processes could not yield eq 11 since straining may increase point defect density, which will be reflected in higher κ_0'. However, τ would not become larger since the jump frequency of a point defect displaced by stress should be higher and the relaxation time should be shorter.

A more direct confirmation of the existence of a charged dislocation mechanism comes from studies on dielectric properties of dislocation-free ice (Itagaki 1978). Anomalously small relaxation spectra with an extrapolated static dielectric constant of about 5 and very short relaxation times (about 1×10^{-6} s at -15°C) indicated that the generally accepted audio frequency dielectric relaxation spectra are caused by the electrically charged dislocation process.

The mechanism discussed above is based on the motion of dislocation segments, both ends of which are fixed by such means as impurities or intersecting dislocations. Corresponding mechanical processes would contribute to internal friction in the low amplitude range. The frequency will be in the audio range at the temperature near the melting point. Experimental results seem to indicate more than one spectrum are affected by mechanical straining (VanDevender and Itagaki 1973). Details of this will be discussed in Part IV.

Though most of the theoretical treatment of charged dislocations has paralleled that for dislocations from internal friction, some difference between internal friction and dielectric relaxation should be realized. Since the Burgers vector of dislocations in a certain direction has either a positive or negative sign, dislocations having a Burgers vector of the opposite sign may interact strongly and their motion may be strongly restricted under the mechanical stress. Generally a crystal contains about equal numbers of positive and negative sign Burgers vector dislocations. Interaction between opposite sign dislocations under the mechanical stress tends to prevent dislocation motion because a change in the distance of the dislocations from the equilibrium position increases the potential energy of interaction.

One dislocation can move in concert with another having the opposite sign Burgers vector without raising interaction energy under the electric field as long as the sign of the charge is the same and moves in the same direction. The dislocation density required to produce known internal friction peaks ($\tan \sigma \cong 0.1$) is four orders of magnitude smaller ($\cong 10^4/m^2$) than the real density observed. The observed density is within one order of magnitude of that required to produce the observed amount of dielectric relaxation if even the lowest charge density is assumed.

In lower frequency ranges and higher fields in which the pinning points would be subjected to higher forces for more prolonged time periods, either the pinning points would eventually start to drift as discussed by Simpson and Sasin (1972), or the dislocation segments would be released from the pinning points. Polarization produced by this means may cause relaxation in a lower frequency range. Neither case would have a direct relationship to creep in mechanical deformation or to d.c. conductivity, both of which would be beyond the capability of the process discussed here.

CONCLUSIONS

Polarization caused by displacement of electrically charged dislocations under an electric field was found to be large enough to be the source of audio frequency dielectric relaxation of ice. The distribution of segment lengths observed in X-ray topographs can explain the deviation from Debye relaxation in dielectric measurements, indicating that the charged dislocation process can be the major source of audio frequency dielectric relaxation. Supporting experimental evidence will be discussed in Part III of this series.

LITERATURE CITED

Bilde-Sörensen, J.B. (1973) Dislocation link length distribution in creep-deformed magnesium oxide. *Acta Metallurgica*, vol. 21, p. 1495–1501.

Bjerrum, N. (1951) Structure and properties of ice: I. The position of the hydrogen atoms and the zero point entropy of ice. *K. Danske Vidensk. Selesk. Skr.*, vol. 27, p. 1–56.

Brantley, W.A. and C.L. Bauer (1969) Effect of charged dislocations on dielectric, piezoelectric and elastic properties. *Material Science and Engineering*, vol. 4, p. 29–38.

Fukuda, A. and A. Higashi (1969) X-ray diffraction topographic studies of dislocations in natural large ice single crystals. *Japanese Journal of Applied Physics*, vol. 8, p. 993–999.

Granato, A. and K. Lucke (1956) Theory of mechanical damping due to dislocations. *Journal of Applied Physics*, vol. 27, p. 583–593.

Hanson, K. and J.W. Morris, Jr. (1975) Limiting configuration in dislocation glide through a random array of point obstacles. *Journal of Applied Physics*, vol. 46, p. 893–990.

Hirth, J.P. and J. Lothe (1968) *Theory of dislocations*, p. 425. New York: McGraw-Hill.

Hobbs, P.V. (1974) *Ice physics.* London: Oxford University Press, chapter 2.

Itagaki, K. (1969) Contribution of charged dislocation motion on dielectric behavior of ice. *Bulletin of the American Physical Society*, series III, vol. 14, no. 3, p. 411.

Itagaki, K. (1978) Dielectric properties of dislocation-free ice. *Journal of Glaciology*, vol. 21, p. 207–217.

Itagaki, K. (1979) Charged dislocation in ice: I. Existence and charge density measurement by X-ray topography. CRREL Report 79-25. ADA078775.

Jonscher, A.K. (1975) Physical basis of dielectric loss. *Nature*, vol. 253, p. 717–719.

Koehler, J.S. (1952) The influence of dislocation and impurities on the damping and the elastic constants of metal single crystals. In *Imperfection in nearly perfect crystals* (W. Schockley et al. Eds.), New York: Wiley, p. 197–216.

Kuroiwa, D. (1965) Internal friction of H_2O, D_2O and natural glacier ice. CRREL Research Report 131. AD615732.

Labusch, R. (1977) Statistical theory of dislocation configurations in a random array of point obstacles. *Journal of Applied Physics*, vol. 48, p. 4550–4556.

Simpson, H.M. and A. Sasin (1972) Contribution of defect dragging to dislocation damping: I. Theory. *Physical Review B.*, vol. 5, p. 1382–1393.

VanDevender, J.P. and K. Itagaki (1973) Internal friction of single-crystal ice. CRREL Research Report 243. AD759930.

von Hippel, A., D.B. Knoll and W.B. Westphal (1971) Transfer of protons through "pure" ice. *Single crystals: I. Polarization spectra of ice,* In *Journal of Chemical Physics*, vol. 54, no. 1, p. 134–144.

APPENDIX A. MOSOTTI TYPE CATASTROPHE BY CHARGED DISLOCATION PROCESSES

Because of the linear charge array on the dislocation line, the Mosotti field on the charged dislocation has to be modified from the original Mosotti relationship, $E' = (\kappa_0 + 2)\cdot E_0/3$ to $E' = (\kappa_0' + 1)\,E_p/2$, according to the eq A5 of Part I (Itagaki 1979). Therefore eq 8 becomes

$$\kappa_0' = 1 + F(\kappa_0' + 1)/2 \tag{A1}$$

where

$$F = \frac{8\mu^2 \Lambda L^2}{\pi^3 C E_v} .$$

Solving for κ_0' we obtain

$$\kappa_0' = \frac{2 + F}{2 - F} . \tag{A2}$$

Therefore κ_0' goes to infinity when $K = 2$, a catastrophe, as appeared here. Using the values obtained from Part I, we obtain F values at 455, 50.5, and 0.2, with values of $\mu = 1.5 \times 10^{-10}$, 0.5×10^{-10} and 3.2×10^{-12} C/m respectively. Those are within the possible range for finding catastrophes, depending on the various conditions. If we assume that the only variable is mobile dislocation density, a catastrophe will appear at the dislocation density of 2.2×10^6, 2.0×10^7 and $4.8 \times 10^9/m^2$ for the charge density of 1.5×10^{-10}, 0.5×10^{-10} and 3.2×10^{-12} C/m, respectively. These dislocation densities are within the observed range. Hence, the effective field would be reduced at higher frequencies by the relaxation phenomena and some anomaly would be expected to appear in a certain range of dielectric relaxation spectra.

A facsimile catalog card in Library of Congress MARC format is reproduced below.

Itagaki, Kazuhiko
Charged dislocation in ice: II. Contribution of dielectric relaxation / by Kazuhiko Itagaki. Hanover, N.H.: U.S. Cold Regions Research and Engineering Laboratory; Springfield, Va.: available from National Technical Information Service, 1982.
iii, 21 p., illus., 28 cm. (CRREL Report 82-7.)
Prepared for Office of the Chief of Engineers by Corps of Engineers, U.S. Army Cold Regions Research and Engineering Laboratory under DA Project 4A161102AT24.
Bibliography: p. 14.
1. Dielectric strength. 2. Dislocation. 3. Electric charge. 4. Ice. 5. Single crystals. I. United States. Army. Corps of Engineers. II. Army Cold Regions Research and Engineering Laboratory, Hanover, N.H.
III. Series: CRREL Report 82-7.

☆U.S. GOVERNMENT PRINTING OFFICE: 1982—501-006/367

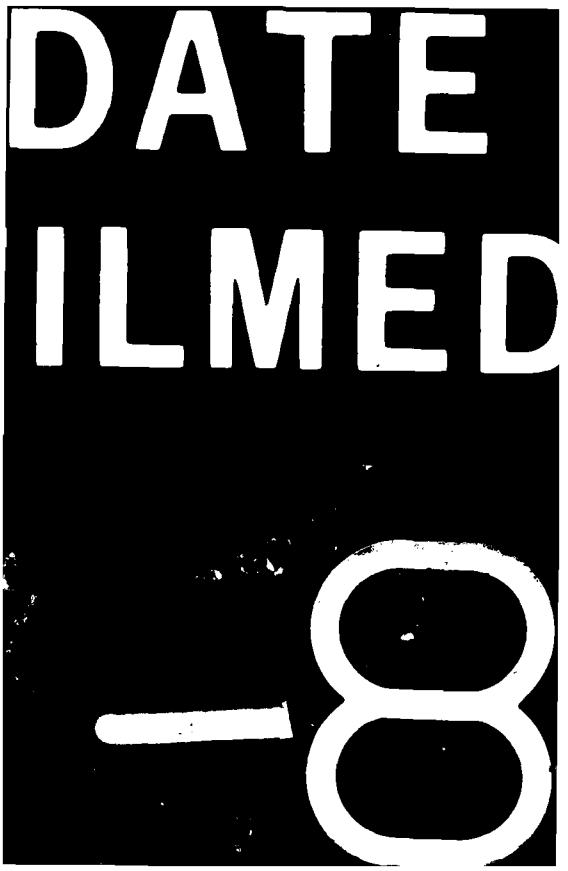
DATE
ILMED
-8